

A critical state interpretation for the cyclic liquefaction resistance of silty sands

George D. Bouckovalas*, Konstantinos I. Andrianopoulos, Achilleas G. Papadimitriou

*Department of Geotechnical Engineering, Faculty of Civil Engineering, National Technical University of Athens,
42 Patission Str. Athens 106 82, Greece*

Abstract

Contrary to many laboratory investigations, common empirical correlations from in situ tests consider that the increase in the percentage of fines leads to an increase of the cyclic liquefaction resistance of sands. This paper draws upon the integrated Critical State Soil Mechanics framework in order to study this seemingly not univocal effect. Firstly the effect of fines on the Critical State Line (CSL) is studied through a statistical analysis of a large data set of published monotonic triaxial tests. The results show that increasing the content of non-plastic fines practically leads to a clockwise rotation of the CSL in ($e-\ln p$) space. The implication of this effect on cyclic liquefaction resistance is subsequently evaluated with the aid of a properly calibrated critical state elasto-plastic constitutive model, as well as a large number of published experimental results and in situ empirical correlations. Both sets of data show clearly that a fines content, less than about 30% by weight, may prove beneficial at relatively small effective stresses ($p_0 < 50-70$ kPa), such as the in situ stresses prevailing in most liquefaction case studies, and detrimental at larger confining stresses, i.e. the stresses usually considered in laboratory tests. To the extent of these findings, a correction factor is proposed for the practical evaluation of liquefaction resistance in terms of the fines content and the mean effective confining stress.

© 2002 Elsevier Science Ltd. All rights reserved.

Keywords: Sand; Silt; Liquefaction; Cyclic loading; Earthquake; Critical state

1. Introduction

The effect of fines on the cyclic liquefaction potential of sands has been studied extensively in geotechnical literature. Still, despite the amount of related research, results seem somewhat contradictory. Namely, mostly empirical correlations from in situ tests show that the presence of fines increases liquefaction resistance [12], while the majority of laboratory tests shows the opposite trend, at least for fines content less than about 30% of total weight [4,16]. The effect of plasticity of the included fines has also stirred contradiction. For example, Koester [4] claims that the plasticity index I_p of fines is less important than the fines content itself, contrary to Refs. [3,10] who claim that fines with high plasticity may fundamentally change the mechanism of excess pore pressure buildup. Nevertheless, this paper does not deal with this issue but focuses on the effect of non-plastic fines content $f(\%)$, which is a relatively complicated issue in itself.

Available interpretations for the effect of fines content on liquefaction resistance are based on mechanisms of deformation in the particle size level. Factors such as soil fabric and aging have been considered responsible for the increase of resistance of undisturbed specimens compared to reconstituted ones [19], and are used to explain why empirical correlations from in situ tests consider the presence of fines as beneficial for liquefaction resistance.

When the effect of aging is being removed, by using reconstituted specimens, micromechanical interpretations of laboratory test results suggest that fines in small percentages ($f < 30\%$) merely take up the space between sand particles without contributing to soil strength. This leads to a decrease of void ratio e without any particular change in soil behavior. In this manner, the decrease in liquefaction resistance with fines content $f(\%)$ is considered an artifact of considering soils with the same e value, and not the same intergranular void ratio of the sand skeleton e_{SK} , a more representative index of behavior [9,14,15,17]. Similarly, for larger $f(\%)$ values, the fines dominate over the sand matrix and the overall behavior depends greatly on the included fines, which contribute their share and lead to an increase in liquefaction resistance.

* Corresponding author. Tel.: +30-210-772-3780; fax: +30-210-772-3428.

E-mail addresses: g.bouck@civil.ntua.gr (G.D. Bouckovalas), kandrian@central.ntua.gr (K.I. Andrianopoulos), loupapas@alum.mit.edu (A.G. Papadimitriou).

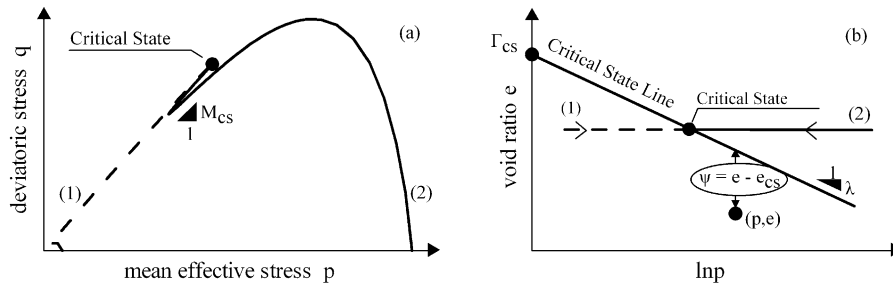


Fig. 1. Effect of initial conditions (e_0, p_0) on monotonic undrained triaxial response of sand in the CSSM context.

These micromechanical explanations provide insight to the phenomenon, but fail to draw the full picture. For example, laboratory results for tests on reconstituted specimens performed at relatively small mean effective stresses, similar to those expected in potentially liquefiable layers at generally shallow depth, show increase of liquefaction resistance with $f(\%)$, which cannot be attributed to aging [18]. This is an indication that the phenomenon is very complicated to be treated merely on the micromechanical level and that it should also be interpreted on the basis of an integrated framework of mechanical behavior.

In an attempt to view this practical issue from a different perspective, the integrated framework of Critical State Soil Mechanics (CSSM), [11] is involved herein. Based on theory as well as on a large amount of available experimental data, this paper identifies the mean effective confining stress p_0 as the missing parameter for the interpretation of the seemingly contradictory evidence that has emerged in the literature. To the extent of this finding, a correction factor is proposed for the liquefaction resistance of low plasticity ($I_p < 5\%$) silty sands, with fines content $f < 30\%$, in terms of the mean effective confining stress.

2. Overview of critical state concepts

As a good approximation, the Critical State Lines (CSL) of a specific soil in the ($e - \ln p$) and the ($p - q$) spaces can be assumed as straight and unique, at least for stresses not causing particle crushing [2]. Uniqueness refers to independence of the CSL from testing conditions, such as

drainage, sample preparation method and strain rate. In this sense, the terms Steady State and Critical State are considered interchangeable. For ease of interpretation, the following presentation of basic critical state concepts uses the triaxial stress–strain space. In other words, all equations and results are presented in terms of the mean effective and deviatoric stresses: $p = (\sigma_v + 2\sigma_h)/3, q = (\sigma_v - \sigma_h)$. It is noted, that subscripts v and h denote the vertical and horizontal planes, respectively.

Fig. 1a and b present the CSL in the ($e - \ln p$) and the ($p - q$) spaces, respectively. These lines are described by the following equations

$$e_{CS} = \Gamma_{CS} - \lambda \ln p \tag{1}$$

$$q = M_{CS} p \tag{2}$$

where e_{CS} is the void ratio at Critical State under mean effective stress p . Furthermore, they show examples of how monotonic undrained behavior of sand is influenced by initial conditions, i.e. the values of p and e . In an attempt to fully interpret the effect of initial conditions with a single parameter, Been and Jefferies [1] introduced the State Parameter ψ , as

$$\psi = e - e_{CS} \tag{3}$$

It becomes evident, that sand behavior at failure is dilative when $\psi < 0$ and contractive when $\psi > 0$.

Before proceeding with the interpretation of the effect of $f(\%)$ on liquefaction resistance, it is crucial to realize how $f(\%)$ affects the corner stone of the CSSM framework, i.e. the CSL location. For this purpose, Fig. 2a shows the $e - \ln p$ CSL for Kogyuk sand with different $f(\%)$ values [1].

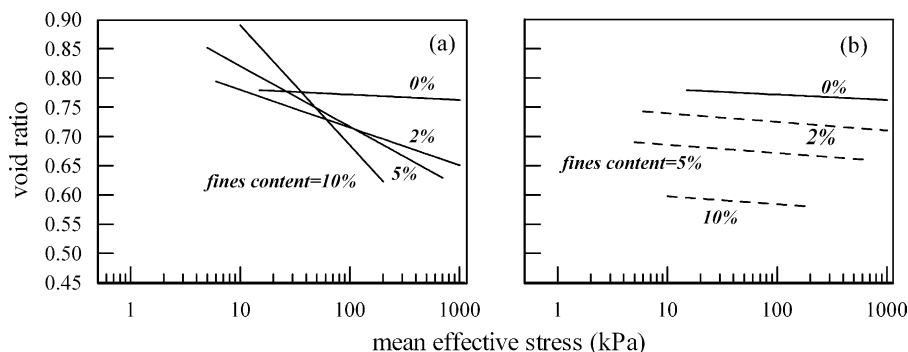


Fig. 2. Effect of fines content on CSL location of Kogyuk Sand; (a) experiments after Ref. [1], and (b) predictions based on the intergranular void ratio concept.

The experimental data show clearly that λ and Γ_{CS} increase as a function of $f(\%)$ or a tendency of the CSL to rotate clockwise around a pivot corresponding roughly to mean effective stresses between 20 and 80 kPa and void ratios between 0.73 and 0.78. This effect of $f(\%)$ implies that increasing the fines content would decrease the tendency for dilation for mean effective stresses greater than that of the pivot and increase it for lower mean stresses. Reasonably, the resulting effect on liquefaction resistance will be similar.

In part at least, this trend of the experimental data contradicts the micromechanical explanation for the effect of fines that is based on the intergranular void ratio, that has been referenced in the introduction. To explain why, Fig. 2b shows the hypothetical CSLs obtained on the basis of the CSL for clean Kogyuk sand ($f = 0\%$) and the following equation that gives the global void ratio e of a given silty sand in terms of the intergranular void ratio e_{sk} of the parent sand, i.e. if the presence of fines is overlooked [15]

$$e = e_{sk} \left(1 - \frac{f(\%)}{100} \right) - f(\%) \quad (4)$$

According to this figure, the CSL in the ($e - \ln p$) space translates almost uniformly towards lower e values with increasing $f(\%)$. Contrary to the experimental data for Kogyuk sand in Fig. 2a, this plot implies that the presence of fines would decrease dilatancy, as well as liquefaction resistance, regardless of the mean effective stress level. In other words, it does not take into account the important role of the mean effective stress in regulating the overall effect of fines.

3. Outline of methodology

This study draws upon the effect of fines on the CSL location shown in Fig. 2a. In the following, this effect is first established with the aid of experimental data from monotonic tests and consequently extrapolated to the liquefaction resistance of silty sands based on theory, as well as on a large number of cyclic liquefaction tests. Table 1 summarizes the tests as well as the basic characteristics of the soils used to study the effect of fines on the CSL location. In all, published data are presented for 42 different parent sands, from various studies and researchers, which were reduced and communicated to the authors by Dr Mike G. Jefferies (Golder Associates UK). In addition, Table 2 outlines the soil characteristics and testing conditions for more than 200 published cyclic liquefaction tests that are used to verify the effect of fines on liquefaction resistance. These data were collected and reduced by the authors.

Extrapolation of the effect of fines on the CSL location to the liquefaction resistance of silty sands, and interpretation of the relevant cyclic test data, was guided by a recently proposed critical state model for cyclic shearing of sands [6,7]. This model explicitly incorporates the state parameter ψ of Ref. [1] in constitutive equations and can provide reasonably accurate

simulations of cyclic liquefaction tests for a wide range of initial (p and e) conditions with a single set of parameters. Furthermore, its selection draws on the fact that the parameters governing the CSL location, i.e. parameters Γ_{CS} , λ and M_{CS} , are user specified and can be consequently varied directly, according to the fines content of the sand.

A total of 90 parametric analyses were performed with this constitutive model for fines content $f = 0, 5, 10, 20$ and 30% and mean effective consolidation stresses $p_0 = 50, 100$ and 200 kPa. The model was calibrated against isotropically consolidated undrained cyclic triaxial tests on Nevada sand ([6,7]). This is a relatively uniform, fine-grained soil that is part of the experimental database used to define the effect of fines on the CSL (Table 1). Typical comparisons between theoretical predictions and experimental results for this soil are shown in Figs. 3 and 4.

Admittedly, using a constitutive model in such a manner is not common, from fear that its use may railroad the interpretation of the test data to false conclusions. The authors' perspective is that this is not the case in this study. The main reason is that the model is actually used here to associate the effects of fines on the CSL location and the cyclic liquefaction resistance in a systematic manner (i.e. provide guidelines), and not to study the liquefaction resistance per se. In other words it is merely the tool to involve the CSSM framework in the interpretation of the cyclic test data.

4. Effect of fines on CSL location

In quantitative terms, this issue is investigated by conducting a statistical analysis of the relevant experimental results addressed in Table 1. Note that the results of the statistical analysis are not intended to replace experiments in the practical definition of the CSL for sands with different fines content $f(\%)$. They are simply used here in order to describe the gross expected trend of how fines affect the location of the CSL in the $p-q$ and the $e-p$ spaces, at least for sands that are similar to the ones in the relevant database.

The results of the statistical analysis of the raw data for Γ_{CS} , λ and M_{CS} in terms of $f(\%)$ are presented in Fig. 5. Despite the scatter of the data, it is observed that both Γ_{CS} and λ increase with $f(\%)$, while M_{CS} could be practically considered constant with an average value of $M_{CS} = 1.26$. The empirical relations between Γ_{CS} , λ and fines content $f(\%)$ are the following

$$\lambda = 0.018 + 0.0027f(\%) \quad (5)$$

$$\Gamma_{CS} = 0.863 + 0.011f(\%) \quad (6)$$

If empirical relations (5) and (6) are combined, they lead to the following direct relation between Γ_{CS} and λ

$$\Gamma_{CS} = 0.79 + 4.1\lambda \quad (7)$$

As shown in Fig. 6, the above equation fits well the raw data ($R = 0.83$), so that it may be considered reliable for a wide

Table 1
Summary of the experimental data used to assess the effect of fines content on the CSL location

Soil	D_{50} (μm)/ f (%)	Number of tests ^a	φ_{cs}^b (deg)	Γ_{SS}	λ_{SS}	Preparation method ^c
AMAULIGAK I-65	290/3	4 + 6	31.8	1.023	0.041	MC
AMAULIGAK I-65	310/9	3 + 6	32.3–32.5	1.018	0.066	MC
AMAULIGAK I-65	80/48	4 + 5	31.6–35	1.634	0.155	MC
AMAULIGAK F-24	140/10	3 + 6	31.6–34	0.946	0.036	MC
AMAULIGAK F-24	144/21	3 + 8	32.8–33	0.966	0.054	MC
BANDING #1	176/0	0 + 5	30	0.830	0.011	MC
BANDING #5	114/1.5	0 + 4	30	0.880	0.020	MC
BANDING #6	157/0	0 + 37	30	0.810	0.017	MC
BANDING #9	142/0	0 + 2	30	0.820	0.013	MC
BEAUFORT	140/5	7 + 13	30.5–31	0.910	0.016	MC&DP
BEAUFORT	140/10	7 + 9	30–30.5	0.920	0.023	MC&DP
CASTRO-B	150/0	12 + 27	30.5	0.791	0.018	MC
CASTRO-C	280/0	4 + 12	34	0.988	0.017	MC
ERKSAK	330/0.7	15 + 8	30–31.5	0.824	0.013	MC&WP
ERKSAK	320/1	5 + 7	31.5	0.875	0.019	MC&WP
ERKSAK	320/2	0 + 5	?	0.910	0.028	MC&WP
ERKSAK	355/3	5 + 7	29.5	0.848	0.023	MC&WP
HOKKSUND	390/0	17 + 5	32	0.934	0.023	MC
ISSERK	230/1	0 + 8	31.6	0.870	0.017	MC
ISSERK	210/2	5 + 5	30.5	0.833	0.019	MC
ISSERK	210/5	5 + 8	31	0.879	0.039	MC
ISSERK	210/10	5 + 5	31–31.5	0.933	0.053	MC
KOGYUK	350/0	0 + 10	32.3	0.79	0.004	MC
KOGYUK	350/2	8 + 13	32.5	0.844	0.028	MC
KOGYUK	350/5	12 + 11	32.5	0.924	0.045	MC
KOGYUK	280/5	5 + 4	30	0.902	0.027	MC
KOGYUK	350/10	6 + 7	30–31	1.095	0.089	MC
LEIGHTON BUZZARD	120/5	6 + 0	31	0.972	0.023	MC
LEIGHTON BUZZARD	880/0	0 + 2		0.940	0.038	MC
MONTEREY	370/0	22 + 5	32	0.878	0.013	MC
NERLERK	300/1	6 + 0	30.5	0.849	0.021	MC
NERLERK	280/2	0 + 8	?	0.882	0.017	MC
NERLERK	280/12	0 + 7	?	0.835	0.030	MC
NEVADA	150/7.5	10 + 0	30	0.910	0.020	DP
OTTAWA	530/0	6 + 5	28.5	0.754	0.012	MC
REID BEDFORD	240/0	5 + 6	32	1.014	0.028	MC
TICINO-4	530/0	5 + 6	31	0.986	0.024	MC
TICINO-8	530/0	5 + 5	31	0.943	0.013	MC
TICINO-9	530/0	5 + 5	31	0.970	0.022	MC
TOYOURA	160/0	10 + 5	30.9	0.879	0.039	MC
TOYOURA	210/0	4 + 5	30.9	1.000	0.017	MC
UKALERK	300/0.8	0 + 4	?	0.830	0.022	MC

^a Number of drained + undrained tests.

^b Range represents the difference between drained and undrained tests.

^c MC: moist compaction; WP: wet pluviation; DP: dry pluviation.

range of silty sands. Combining Eqs. (1) and (7) leads finally to the following empirical relation

$$(e - 0.79) = \lambda(4.1 - \ln p) \quad (8)$$

Eq. (8) yields the gross CSL locations for all considered soil types as a function of the corresponding slope λ . Moreover, it suggests that all CSL pass through a pivot point ($p_{\text{piv.}} = e^{4.1} \approx 60$ kPa, $e_{\text{piv.}} = 0.79$), independent of the value of λ . This is shown in Fig. 7 where the average CSLs predicted from Eqs. (8) and (5) are plotted in the $e - \ln p$ space for various values of f (%). Thus, the trend identified earlier for Kogyuk sand (Fig. 2a) appears now to be more generally valid.

Note that, due to objective difficulties related with the definition of the CSL and the statistical analysis itself, the existence of a single pivot point established herein should be regarded as a neat simplification rather than as a physical material property, even for a given parent sand. Nevertheless, this simplification provides valuable insight to the phenomenon and prepares the ground for a rational evaluation of the relative effect of fines on the liquefaction resistance.

5. Effect of fines on liquefaction resistance

From Fig. 7 it is deduced, that two soil samples with the same initial conditions (p_0, e_0) but with different content of

Table 2
Summary of experimental studies used to assess the effect of fines content on cyclic liquefaction resistance

Reference	No. of tests ^a	Initial conditions		Soil characteristics		Preparation method
		p_0 (kPa)	e_0	Parent sand	Fines	
Koester [4]	129 Cy-UTX	103.4 and 206.85	0.69	Fine grained sand ($D_{50} = 0.18$ mm and $C_u = 2.3$)	Uniform silt (PI < 5%, $w_L = 28\%$ and $w_P = 24\%$)	Reconstituted, moist compaction
		103.4 and 206.85	0.59	Medium sand ($D_{50} = 0.48$ mm and $C_u = 1.8$)	Uniform silt (PI < 5%, $w_L = 28\%$ and $w_P = 24\%$)	
		103.4 and 206.85	0.55	Medium sand ($D_{50} = 0.48$ mm and $C_u = 1.8$)	uniform silt (PI < 5%, $w_L = 28\%$ and $w_P = 24\%$)	
		103.4 and 206.85	0.47	Well-graded sand ($D_{50} = 0.45$ mm and $C_u = 5.7$)	uniform silt (PI < 5%, $w_L = 28\%$ and $w_P = 24\%$)	
Troncoso [16]	19 Cy-USS	196	0.85	Tailing sand	Silt	Reconstituted, slurry deposition
Vaid [17]	13 Cy-UTX	350	0.45–0.80	Well-graded 20/200 angular tailing Brenda sand ($D_{50} \approx 0.23$ mm and $C_u \approx 3.3$)	Non-plastic silt	
Polito [8]	6 Cy-UTX	100	0.76	Yatesville sand, subangular to subrounded ($D_{50}=0.18$ mm and $C_u \approx 3.1$)	Non-plastic silt ($D_{50}=0.030$ mm and $C_u \approx 4.4$)	Reconstituted, moist compaction
Polito and Martin [9]	6 Cy-UTX	100	0.68	Monterey sand, subangular to subrounded ($D_{50}=0.43$ mm and $C_u \approx 1.7$)	Non-plastic silt ($D_{50}=0.030$ mm and $C_u \approx 4.4$)	Reconstituted, moist compaction
Kondoh et al. [5]	15 Cy-UTX	50		Sengeniyama sand	Kaolin	Reconstituted ^b
Yasuda et al. [18]	15 Cy-UTX	49	D_r : 30–90%	$D_{50}=0.11–0.50$ mm	Low-plasticity (PI < 5%)	

^a Cy-UTX, cyclic undrained triaxial test; Cy-USS, cyclic undrained simple shear test.

^b Data with $f > 30\%$ or $D_{50} > 0.5$ mm have been omitted.

fines $f(\%)$ correspond to different ψ values. For example, a sample of silty sand ($f \neq 0\%$) with $p_0 < 60$ kPa is expected to behave in a more dilative manner than a clean sand sample ($f = 0$), consolidated to the same initial conditions. As a result, the clean sand sample is expected to exhibit lower cyclic liquefaction resistance due to the relatively smaller $|\psi|$ value. In this context, the effect of $f(\%)$ on liquefaction resistance is reversed for samples with relatively large mean effective stresses ($p_0 > 60$ kPa). In

other words, liquefaction resistance is expected to increase with $f(\%)$ for relatively low mean effective stresses and decrease for relatively high stresses.

The above qualitative conclusions are further substantiated from analytical simulations of cyclic triaxial liquefaction tests on clean Nevada sand ($f = 0\%$) and hypothetical mixtures of the same sand with silt at $f = 5, 10, 20, 30\%$. The values of Γ_{CS} , λ and M_{CS} that are used for the simulations were defined according to Fig. 5 and Eqs. (5) and (6). Three

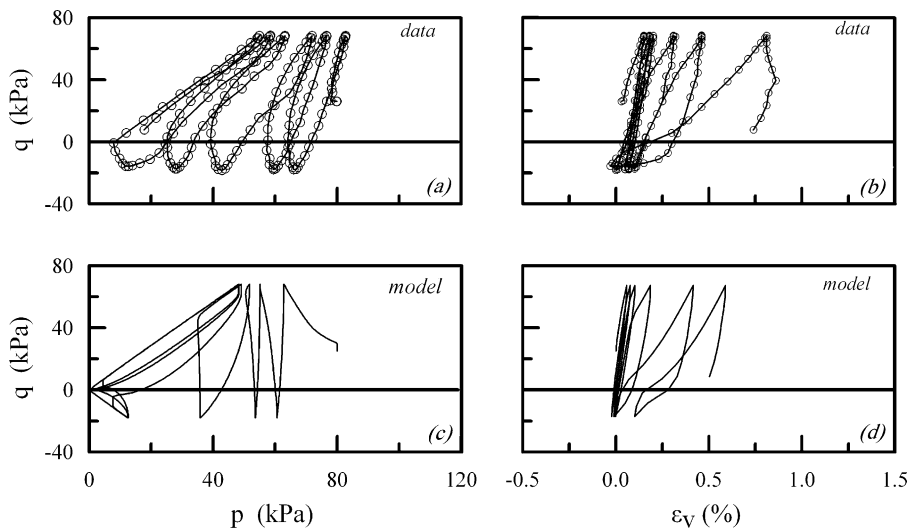


Fig. 3. Detailed comparison of model simulations to data from cyclic liquefaction triaxial tests on clean Nevada sand: (a,c)effective stress path; (b,d)stress–strain relation (from Ref. [6]).

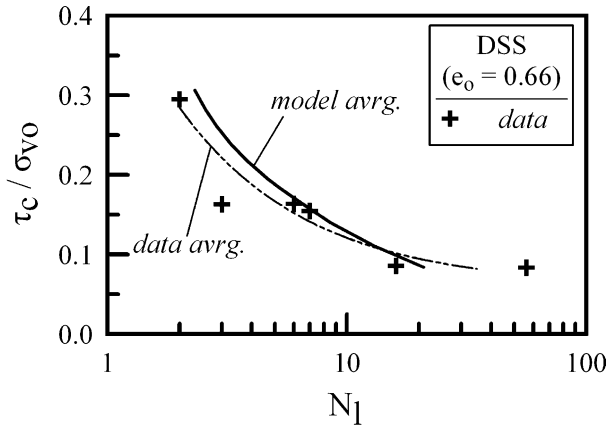


Fig. 4. Average liquefaction curves deduced from simulations and data from 14 cyclic liquefaction simple shear tests on clean Nevada sand [7].

sets of analyses are performed for each soil type, one with $p_0 = 50$ kPa, i.e. to the left of the pivot point, and two with $p_0 = 100$ and 200 kPa, i.e. to the right. The same void ratio is used for all analyses, $e_0 = 0.70$, a value corresponding to medium dense, potentially liquefiable, sands.

The results of the analyses for $p_0 = 50$ and 100 kPa are shown in Fig. 8a and b, in the form of common liquefaction resistance curves. It is noted that cyclic stress amplitude q_c in this figure refers to the amplitude of $|\Delta\sigma_v|/2$ applied within each loading cycle. Observe that the non-univocal trend regarding the effect of fines on cyclic liquefaction resistance that was inferred earlier from experimental data, is fully verified by the analytical simulations. Namely, the simulations for low p_0 values show that cyclic liquefaction

resistance increases when fines are added to the clean sand. On the contrary, simulations for relatively high p_0 values show that the effect of fines is reversed.

Laboratory evidence of this reversing trend is presented in Fig. 9a and b, where the effect of $f(\%)$ on cyclic liquefaction resistance is demonstrated with the aid of element tests consolidated at $p_0 = 49$ and 196 kPa, respectively [5,16]. More specifically, in Fig. 9a tests with low mean confining stress ($p_0 = 49$ kPa) show that increasing $f(\%)$ leads to an increase of the cyclic liquefaction resistance, while in Fig. 9b tests with large mean effective stress ($p_0 = 196$ kPa) show the opposite effect. The beneficial effect of $f(\%)$ on liquefaction resistance from in situ test correlations can also be interpreted in this context. As it is discussed in later paragraphs, these results originate from liquefiable layers close to the ground surface, with the majority of case studies corresponding to mean effective consolidation stress $p_0 = 20$ – 80 kPa [12,13,20].

6. A correction factor for the effect of fines

The effect of fines on liquefaction resistance can be expressed through a correction factor I_f , defined as

$$I_f = CSR_{f \neq 0} / CSR_{f=0} \tag{9}$$

where $CSR_{f=0}$ and $CSR_{f \neq 0}$ are the cyclic stress ratios required to cause liquefaction after a given number of cycles N_1 , for a clean sand and a silty sand, respectively, at the same void ratio.

Fig. 10a and b show the relation between I_f and fines content $f(\%)$ deduced from the analytical predictions presented in Fig. 8 and the experimental data presented in

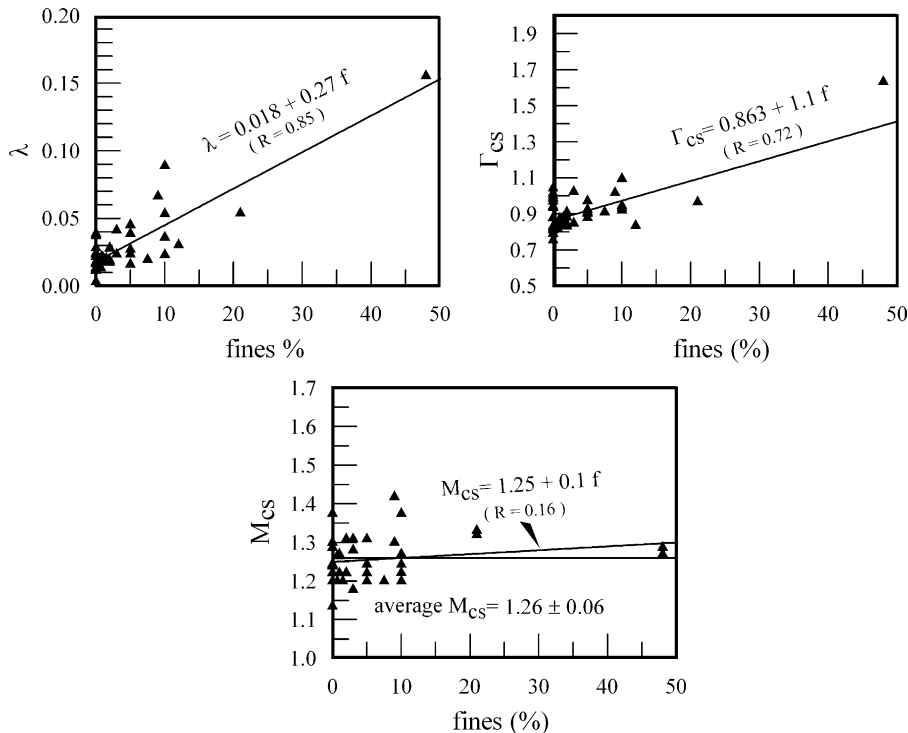


Fig. 5. Statistical evaluation of the effect of fines content on CSL parameters Γ_{cs} , λ and M_{cs} .

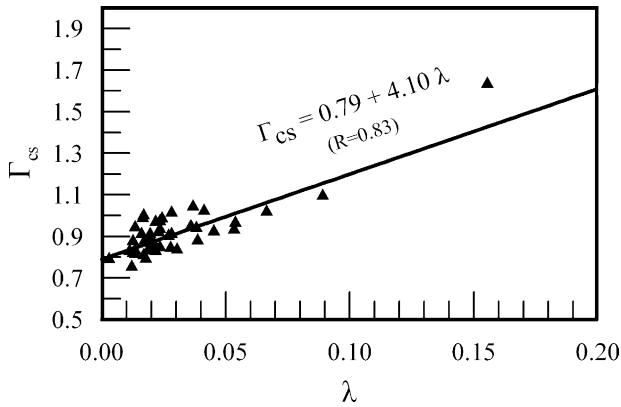


Fig. 6. Correlation between CSL parameters Γ_{cs} and λ .

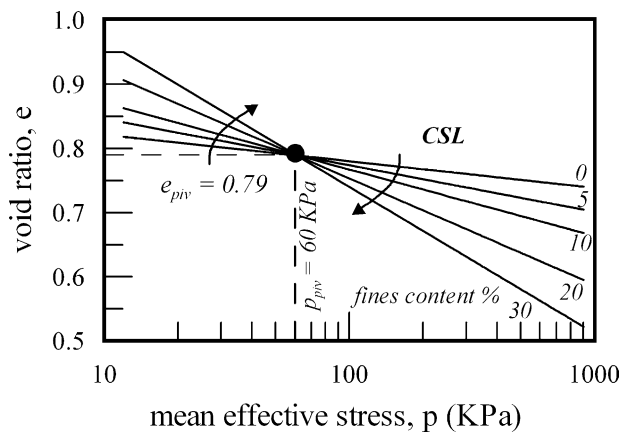


Fig. 7. Idealized effect of fines content on CSL in the $(e - \ln p)$ space.

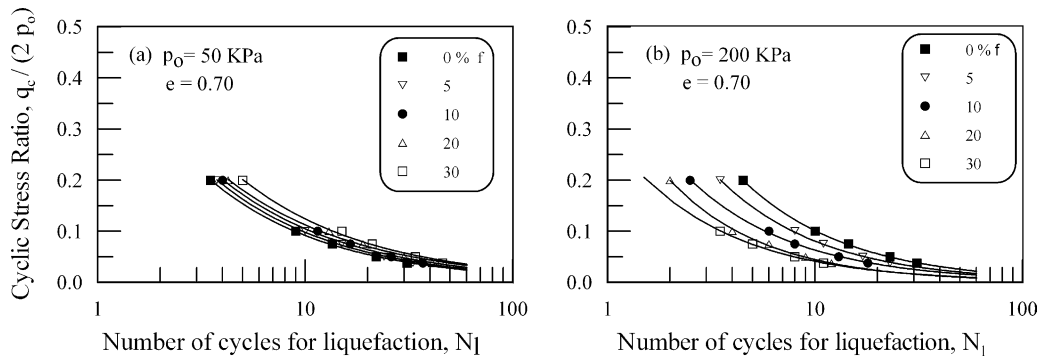


Fig. 8. Theoretical simulation of the effect of fines content on the cyclic liquefaction resistance of Nevada sand; (a) $p_0 = 50$ kPa; (b) $p_0 = 200$ kPa.

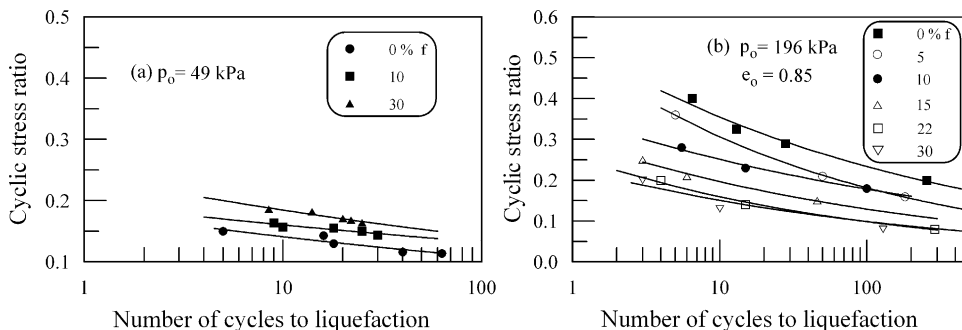


Fig. 9. Experimental results for the effect of fines content on the cyclic liquefaction resistance of sand; (a) $p_0 = 49$ kPa [5]; (b) $p_0 = 196$ kPa [16].

Fig. 9. In both figures, the data points refer to different numbers of cycles to liquefaction N_L . There are two points of interest here: (a) theoretical and experimental values of I_f vary more or less linearly with the content of fines $f(\%)$, and (b) I_f is practically independent of the number of cycles to liquefaction N_L . Additional insight to the correction factor I_f is provided in Fig. 11, that is based on experimental results for Brenda 20/200 sand reported by Vaid [17]. In this figure the variation of I_f with fines content $f(\%)$ is shown for five different values of void ratio, ranging between 0.47 and 0.75. Observe again the linear relation between I_f and $f(\%)$, but also that the variation of I_f is essentially independent of the void ratio.

Following the above observations, I_f is approximately expressed as a linear function of $f(\%)$, i.e.

$$I_f = 1 + \alpha_f \frac{f(\%)}{100} \tag{10}$$

where the parameter α_f depends only on the initial consolidation pressure p_0 . According to the mechanism adopted herein for the interpretation of the effect of fines, α_f should be positive (increase of liquefaction resistance) for $p_0 < p_{piv}$ and negative (decrease of liquefaction resistance) for $p_0 > p_{piv}$.

The dependence of α_f on p_0 is shown in Fig. 12, following reduction and evaluation of the detailed results of the laboratory studies outlined in Table 2, and the recently established empirical relation between liquefaction resistance of silty sands and corrected standard penetration blow count $N_{1,60}$ [20]. The $I_f - f$ relations

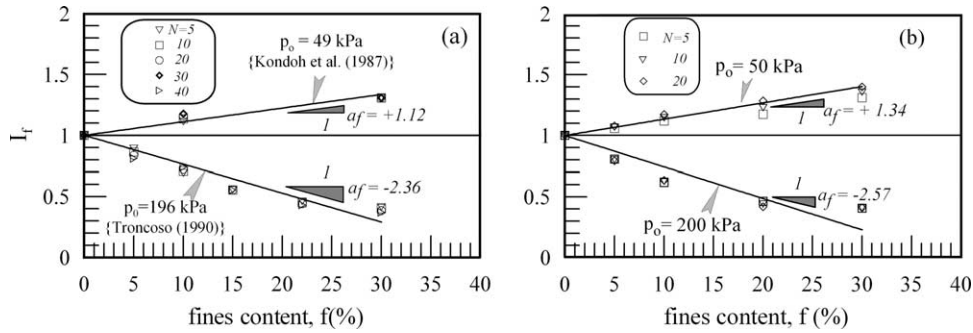


Fig. 10. Variation of correction factor I_f for different mean consolidation stresses and number of cycles to liquefaction: (a) theoretical predictions; (b) experimental data.

from all available experimental data and empirical relations, that were used to estimate the various a_f values are included in the Appendix A.

The procedure used for estimating the correction factor a_f from the empirical relations in terms of $N_{1,60}$ was the same as for the experimental data, only that now calculations were made for constant $N_{1,60}$ instead of constant void ratio e . The calculations were made for earthquake magnitude $M_w = 7.5$, i.e. a constant equivalent number of cycles, and three values of $N_{1,60}$ ($= 5, 10$ and 15) covering the majority of data points used to draw the empirical curves. According to the detailed presentation of the field data by Stark and Olson [13], most of the relevant case studies refer to shallow sand deposits with mean effective confining stresses between 20 and 80 kPa. Thus, computed a_f values were approximately assigned to $p_0 = 52$ kPa, i.e. the statistical median value of all reported mean confining stresses.

According to the experimental data, α_f degrades asymptotically with p_0 , from about (2 ± 1) at $p_0 = 50$ kPa to (-3.5 ± 1) at $p_0 \approx 300$ kPa. The transition from positive to negative values occurs for $p_0 = 50\text{--}70$ kPa, i.e. in the vicinity of the consolidation pressure of the CSL pivot point $p_{piv.} = 60$ kPa. This coincidence provides indirect support to the explanation provided herein for the effect of fines since the monotonic test data used to estimate p_{piv} at first place are totally independent of the cyclic test data used to establish the variation α_f in Fig. 12.

In analytical form, the mean value of α_f in Fig. 12 may be expressed as

$$a_f \approx \left(\frac{p}{p_a}\right)^{-2.50} - 3.50 \quad (11)$$

where p_a denotes the atmospheric pressure ($p_a \approx 100$ kPa).

7. Summary and conclusions

The main points and conclusions drawn from this study are the following:

(a) The effect of fines content $f(\%)$ on liquefaction resistance is a topic of debate in the literature. However, it has been shown herein that the CSSM theoretical

framework can readily explain the different, seemingly contradictory evidence and views.

(b) According to experimental evidence, as the content of fines increases, the CSL in the $(e-\ln p)$ space rotates clockwise around a more or less constant pivot point, with coordinates $e_{piv.} \approx 0.79$ and $p_{piv.} \approx 60$ kPa. The existence and the coordinates of this pivot point were identified on the basis of monotonic shearing tests and indirectly verified with the aid of cyclic liquefaction test data.

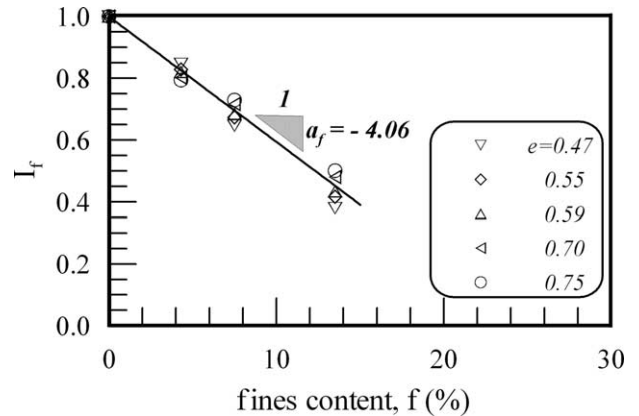


Fig. 11. Experimental values of I_f for Brenda 20/200 sand at different void ratios [17].

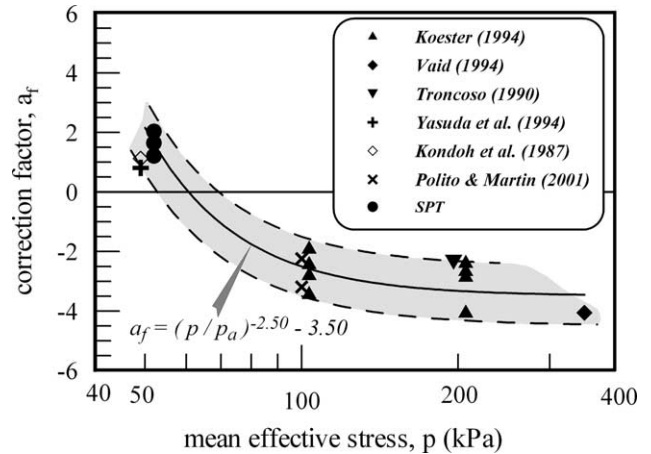


Fig. 12. Variation of correction factor parameter α_f in terms of mean effective confining stress.

(c) The mechanism described above implies that the effect of fines on liquefaction resistance is not univocal, but varies depending upon the level of the mean effective consolidation stress p_0 : in the presence of fines, the resistance to liquefaction increases for $p_0 < p_{piv} = 50\text{--}70$ kPa and decreases for $p_0 > p_{piv}$. This conclusion is verified by cyclic liquefaction test data published in the literature as well as analytical predictions based on critical state soil plasticity.

(d) The effect of fines on the cyclic liquefaction resistance, at any given number of cycles to liquefaction N_L and void ratio e_0 , can be expressed through a correction factor $I_f = 1 + \alpha_f f$, where α_f may be positive or negative depending upon the level of consolidation pressure p_0 . This correlation is given in Fig. 12, based on data from published experimental studies and in situ empirical relations.

Note that the above findings apply to non-plastic sand and silt mixtures with fines content less than about 30%. This limitation draws upon the soil characteristics associated to the monotonic test data that were used to establish the effect of fines on the CSL and the cyclic test data that were used to study the liquefaction resistance of silty sands.

The trends presented herein are consistent and clear, despite the fact that the experimental data come from a large number of independent studies, with different sands and test types. Still, it is expected that they can be considerably refined with the aid of a systematic experimental study,

planned and performed along the basic ideas presented in this paper. A key requirement for that purpose is that the CSL and the cyclic liquefaction resistance are defined for the same parent sands and fines contents so that the link between these two response aspects can be established directly.

Acknowledgements

The authors wish to sincerely thank Dr M.G. Jefferies for the unconditional supply of the monotonic test data used to establish the effect of fines on the location of the CSL, a key issue addressed in the article. The second author, wishes also to acknowledge the financial support provided by the Institute of Communications and Computers of N.T.U.A., as part of the ‘Archimedes’ basic research fund.

Appendix A. Experimental assessment of correction factor I_f

The following figures refer to the assessment of the correction factor I_f , based on the relationships for empirical evaluation of cyclic liquefaction resistance in terms of corrected SPT blow counts $N_{1,60}$ [20], as well as the results of the independent experimental studies outlined in Table 2. For the empirical relations, the figures define the corrected

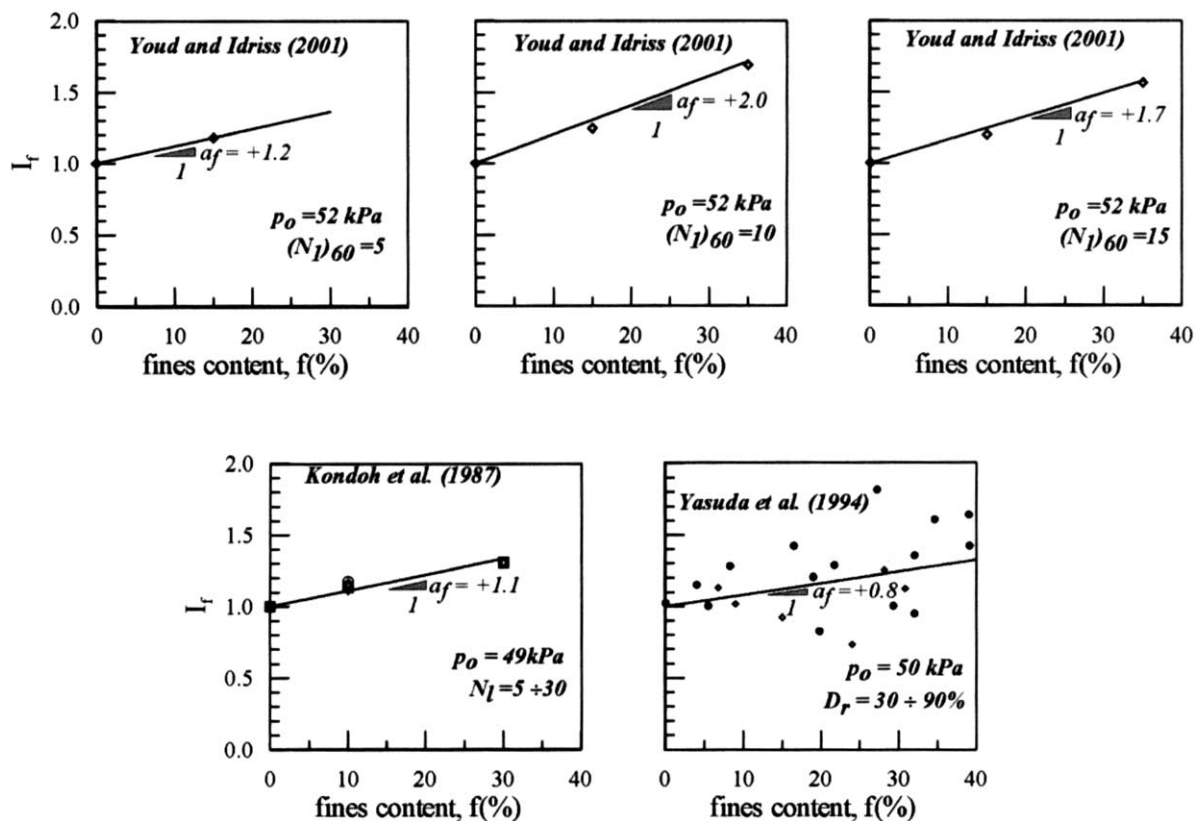


Fig. A1. (a) Liquefaction resistance of clean sand reduced according to Ref. [4] due to membrane compliance.

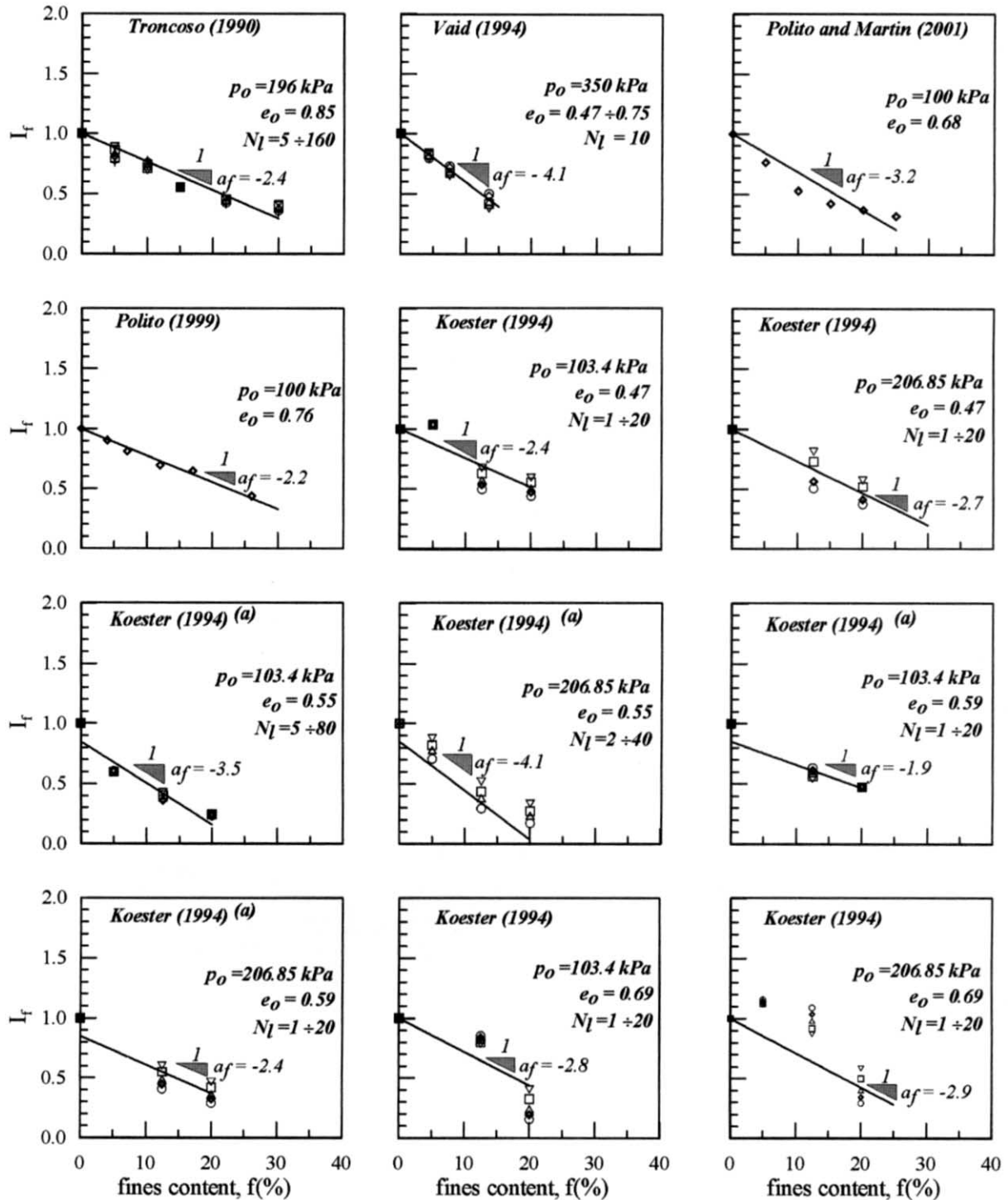


Fig. A1 (continued)

SPT blow counts $N_{l,60}$ and the associated value of the correction factor parameter α_f (Eq. (10)). For the experimental studies, each figure provides the source of the data, the initial conditions of the tests, the number of cycles to liquefaction and the resulting value of the correction factor parameter α_f (Fig. A1).

References

- [1] Been K, Jefferies MG. A state parameter for sands. *Geotechnique* 1985;35(2):99–112.
- [2] Been K, Jefferies MG, Hachey J. The critical state of sands. *Geotechnique* 1991;41(3):365–81.

- [3] Ishihara. Soil behaviour in earthquake geotechnics. Oxford Engng Sci Ser 1993;46.
- [4] Koester JP. In: Prakash S, Dakoulas P, editors. The influence of fines type and content on cyclic strength. Ground failures under seismic conditions, 44. ASCE Publication; 1994. p. 17–33.
- [5] Kondoh M, Sasaki Y, Matsumoto H. Effect of fines content on soil liquefaction strength (Part 1). Proceedings of the Annual Meeting of the JSSMFE. Tsukuba, Japan: Public Works Research Institute, Ministry of Construction; 1987.
- [6] Papadimitriou AG, Bouckovalas G, Dafalias Y. Plasticity model for sand under small and large cyclic strains. J Geotech Geoenviron Engng, ASCE 2001;127(11):973–83.
- [7] Papadimitriou AG, Bouckovalas G. Plasticity model for sand under small and large cyclic strains: a multi-axial formulation. Soil Dyn Earthquake Engng 2002;22:191–204.
- [8] Polito CP. The effect of non-plastic and plastic fines on the liquefaction of sandy soils. PhD thesis. Blacksburg, VA: Virginia Polytechnic Institute and State University; 1999.
- [9] Polito PC, Martin II JR. Effect of nonplastic fines on the liquefaction resistance of sands. J Geotech Geoenviron Engng, ASCE 2001; 127(5):408–15.
- [10] Prakash S, Guo T. Liquefaction of silts and silt–clay mixtures. J Geotech Geoenviron Engng, ASCE 1999;125(8):706–10.
- [11] Roscoe KH, Schofield AN, Wroth CP. On the yielding of soils. Geotechnique 1958;9:71–83.
- [12] Seed HB, Tokimatsu K, Harder LF, Chung RM. Influence of SPT procedures in soil liquefaction resistance evaluations. J Geotech Engng, ASCE 1985;111(12):1425–45.
- [13] Stark TD, Olson SM. Liquefaction resistance using CPT and field case histories. J Geotech Engng 1995;121(12):856–69.
- [14] Thevanayagam S. Effects of fines and confining stress on undrained shear strength of silty sands. J Geotech Geoenviron Engng, ASCE 1998;124(6):479–91.
- [15] Thevanayagam S, Mohan S. Intergranular state variables and stress–strain behaviour of silty sands. Geotechnique 2000;50(1):1–23.
- [16] Troncoso, JH. Failure risks of abandoned tailing dams. Proceedings of International Symposium on Safety and Rehabilitation of Tailing Dams. Paris: International Commission on Large Dams; 1990. p. 82–9.
- [17] Vaid YP. Liquefaction of silty soils. In: Prakash S, Dakoulas P, editors. Ground failures under seismic conditions, 44. ASCE Publication; 1994. p. 1–16.
- [18] Yasuda S, Wakamatsu K, Nagase H. Liquefaction of artificially filled silty sands. In: Prakash S, Dakoulas P, editors. Ground Failures under Seismic Conditions, 44. ASCE Publication; 1994. p. 91–104.
- [19] Yoshimi Y, Tokimatsu K, Hasaka Y. Evaluation of liquefaction resistance of clean sands based on high-quality undisturbed samples. Soils Found 1989;29(1):93–104.
- [20] Youd TL, Idriss IM. Liquefaction resistance of soils: summary report from the 1996 NCEER and 1998 NCEER/NSF workshops on evaluation of liquefaction resistance of soils. J Geotech Geoenviron Engng 2001;127(4):297–313.